

Article

The Study of Heat Treatment Effects on Chromium Carbide Precipitation of 35Cr-45Ni-Nb Alloy for Repairing Furnace Tubes

Nakarin Srisuwan ^{1,*}, Krittee Eidhed ², Nantawat Kreatsereekul ¹,
Trinet Yingsamphanchareon ^{3,4} and Attaphon Kaewvilai ^{3,4}

Received: 30 November 2015; Accepted: 13 January 2016; Published: 19 January 2016

Academic Editor: Hugo F. Lopez

¹ Thai-French Innovation Institute, King Mongkut's University of Technology North Bangkok, Bangsue, Bangkok 10800, Thailand; natthawat.k@tfii.kmutnb.ac.th

² Faculty of Engineering, King Mongkut's University of Technology North Bangkok, Bangsue, Bangkok 10800, Thailand; krittee.eed@gmail.com

³ Department of Welding Engineering Technology, College of Industrial Technology, King Mongkut's University and Technology North Bangkok, Bangsue, Bangkok 10800, Thailand; trinet2518@hotmail.com (T.Y.); attaphonk@kmutnb.ac.th (A.K.)

⁴ Welding Engineering and Metallurgical Inspection, Science and Technology Research Institute, King Mongkut's University and Technology North Bangkok, Bangsue, Bangkok 10800, Thailand

* Correspondence: nakrin.s@tfii.kmutnb.ac.th; Tel.: +66-2-555-2000 (ext. 2534); Fax: +66-2-586-9014

Abstract: This paper presents a specific kind of failure in ethylene pyrolysis furnace tubes. It considers the case in which the tubes made of 35Cr-45Ni-Nb high temperature alloy failed to carburization, causing creep damage. The investigation found that used tubes became difficult to weld repair due to internal carburized layers of the tube. The microstructure and geochemical component of crystallized carbide at grain boundary of tube specimens were characterized by X-ray diffractometer (XRD), scanning electron microscopy (SEM) with back-scattered electrons mode (BSE), and energy dispersive X-ray spectroscopy (EDS). Micro-hardness tests was performed to determine the hardness of the matrix and the compounds of new and used tube material. The testing result indicated that used tubes exhibited a higher hardness and higher degree of carburization compared to those of new tubes. The microstructure of used tubes also revealed coarse chromium carbide precipitation and a continuous carbide lattice at austenite grain boundaries. However, thermal heat treatment applied for developing tube weld repair could result in dissolving or breaking up chromium carbide with a decrease in hardness value. This procedure is recommended to improve the weldability of the 35Cr-45Ni-Nb used tubes alloy.

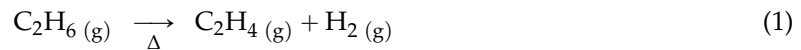
Keywords: ethylene pyrolysis; furnace tube; chromium carbide; heat treatment; carbide dissolution; carburization

1. Introduction

1.1. Material for Ethane Pyrolysis Furnaces Tube

Ethylene (C₂H₄) can be generated by the thermal cracking of ethane (C₂H₆), which is passed through a coil of reaction tubes externally heated to a temperature of 1000–1150 °C in pyrolysis furnaces. The decomposition of ethane into ethylene is represented by the reaction below (1) [1]. Carbon residue from the combustion products can be deposited at the internal surface of the tube wall as adherent coke and must be removed repeatedly via decoking in water vapor and air. Consequently, the internal carbide formation can occur after a corrosion phenomenon called “carburization”, which reduces the

mechanical properties of materials and causes damages [2,3]. Thus, the alloy material must be suitable to accommodate the high process temperature. These alloys are selected for better high creep strength, carburization resistance, thermal shock resistance and weldability.



The Ni-Cr-Fe alloys are known for producing material for tubular coils within an industrial pyrolysis furnace. They have been developed for using at elevated temperature where relatively severe mechanical stresses are encountered and high surface stability is required [4]. The structure of Ni-Cr-Fe alloys consist of the primary phase of γ austenitic FCC matrix (Figure 1a), plus a variety of secondary phases [5], which are the metal carbides denoted only by the compound M_xC such as MC , M_6C and M_{23}C_6 (M = Metals, C = carbide), as shown in Figure 1b.

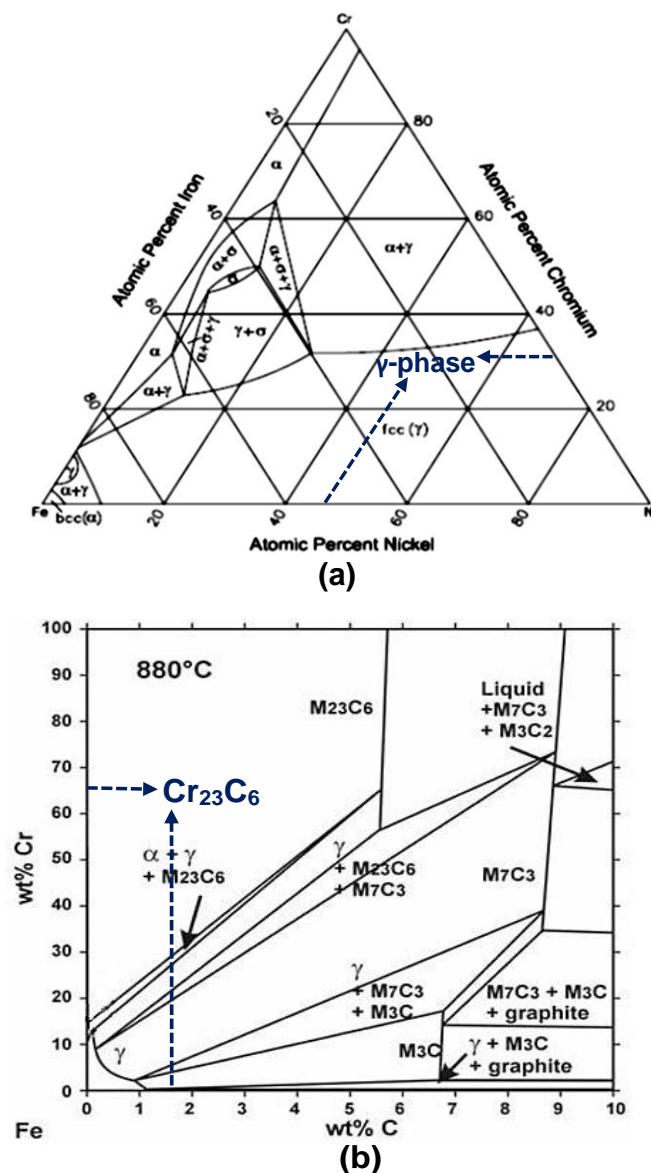


Figure 1. Phases of 35Cr-45Ni-Fe alloy: (a) primary γ -phase; and (b) secondary carbides phase.

Previously, the small additions of niobium (Nb) to the tube production were able to increase their resistance to thermal shock, while the Nb acts as a carbide stabilizer. Moreover, the nickel and

niobium could be combined in the matrix of an alloy to form body-centered tetragonal (BCT) called the metastable γ'' -Ni₃Nb phase. This phase provides very high strength at low and intermediate temperatures; however, it is unstable at high temperatures above 650 °C [6,7].

The transition of carbides in the Ni-Cr-Fe alloys can be considered by the Ellingham diagram (relation between temperatures and Gibbs free energy; ΔG) [8]. In the range of temperatures over 850 °C, the ΔG of nickel carbide and iron carbide (Ni₃C and Fe₃C) are positive such that the formation of these carbides are a nonspontaneous process. On the other hand, the ΔG of chromium and niobium are negative, which indicates that the chromium and niobium tend to combine with carbon to form chromium carbides (Cr₂₃C₆ or Cr₇C₃) and niobium carbide (NbC and Nb₂C), called carbide precipitation or sensitization [9]. The type of formed carbide depends on the contents of the metal and carbon in the alloy. Moreover, the precipitation of silicon carbide (SiC) has also occurred in the structure of Ni-Cr-Fe alloys, but temperature is a very important factor in the determination of which polytype of SiC is formed [6].

From the carbide precipitation, the corrosion resistance of Ni-Cr-Fe alloy decreased while the hardness and brittleness were increased [10]. The change in microstructure and in the properties of the Ni-Cr-Fe alloy is a serious problem in the repairing of tube furnaces by welding.

1.2. Weldability with Thermal Heat Treatment

In general, post-weld heat treatments (PWTH) are usually not required for the non-precipitation-hardenable Ni-Cr-Fe alloy weldments except for an additional agreement between the owner and the welding contractor. However, in dissimilar-metal welding (DMW), the identity and properties of the two metals being joined, and of the filler metal joining them, must be considered. For example, if the Ni-Cr-Fe alloy being joined has various different physical and metallurgical properties after long-term service, preheat should be used to make a dissimilar-metal weld. Another variable that should be considered might be the need for a post-heat treatment for reducing the weldability problems from different materials [11]. Additionally, the formation of chromium carbides is readily reversed by thermal heat treatment [9,12]. Therefore, the tubing repair process could consider a dissimilar-metal weld as well as a pre-heat treatment as an important parameter. The failure of the Ni-Cr-Fe alloy in the petrochemical industry has been studied, and the influence of carburization, carbide formation, thermal treatment conditions and welding repair technology has been investigated by some researchers [1–3,13–19].

However, this study is related to the problems of the weld repair process of used tubes in ethylene pyrolysis furnace from the petrochemical industry in Thailand. The failure analysis was performed via visual inspection and hardness measurements of the used tubes. Chromium carbide precipitation was investigated. The results obtained provide guidance on applications of weld repair procedures when the Ni-Cr-Fe alloy tube has a difference level of carburization.

2. Materials and Methods

2.1. Material Verification

A Ni-based super alloy 35Cr-45Ni-Nb grade (Elemental composition: 45% Ni, 35% Cr, 14.5% Fe, 1.8% C, 1.7% Si, 1% Nb and 1% Mn) was used as a material. This alloy does not belong to the standardized ASME-II Part B code (Non-ferrous metal); however, it was typically used in carburizing applications. The information and visual inspection of experimental material are shown in Table 1.

Table 1. Information of 35Cr-45Ni-Nb tube specimen and visuals inspection.

Specimen	Information and Visual Inspection		Image
Tube No. 1 (New)	Diameter (OD)	63.4 ± 0.2 mm	
	Outside wall	Light gray shade	
	Inside wall	Original smooth surface	
	Visual inspection	No coke deposit, original roundness, no swell	
Tube No. 2 (Used)	Location	9 m on the ground	
	Diameter (OD)	67.8 ± 0.8 mm	
	Outside wall	Black shade & rough surface	
	Inside wall	Thin coke deposit	
Tube No. 3 (Used)	Location	2 m on the ground	
	Diameter (OD)	65.0 ± 0.4 mm	
	Outside wall	Black shade & rough surface	
	Inside wall	Thin coke deposit	
Tube No. 4 (Used)	Location	1 m on the ground	
	Diameter (OD)	65.0 ± 0.4 mm	
	Outside wall	Black shade & rough surface	
	Inside wall	Thin coke deposit inside tube	
	Visual inspection	Near original roundness	

Specimen No. 1 and used tubes No. 2–4 (after 6 years of service at pressure 32 bar, and a temperature of about 800–1100 °C) were carefully cut into the outside diameter at 6.3–6.8 cm and 1.0 cm of thickness. After that, the new tube and used tubes were analyzed by an X-ray diffractometer, (XRD: Philips X-Pert-MPD, Eindhoven, The Netherlands), a scanning electron microscope (SEM: JEOL JSM-6310F, Peabody, MA, USA) with back-scattered electrons mode (BSE), and an energy-dispersive X-ray spectrometer (EDS: EDAX, New York, NY, USA) with elemental mapping.

2.2. Heat Treatment, Hardness and Microstructure

The heat treatments of specimens were performed in three conditions, as reported in Table 2. The specimens before (No. 1) and after heat treatment (No. 2–4) were tested by the Vickers micro-hardness testing and further analyzed the microstructure by combining techniques of SEM-BSE and EDS mapping.

Table 2. Heat treatment conditions.

Conditions	Heat Treatment Methods		Note
C1	Without heat treatment		New tube (No. 1)
C2	Pre-heat 600 °C, 1 h	Cooled down in air	Used tube (No. 2–4)
C3	Pre-heat 900 °C, 1 h	Cooled down in air	Used tube (No. 2–4)

For hardness testing, each of specimen was divided into four quadrants (area 1–4) for comparing the hardness at different position on the cross sectional areas as shown in Figure 2. During the micro-hardness testing, all specimens corresponded to the NACE Standard TM 0498-98 and ASTM A370, with accepted load settings of 500 kg.

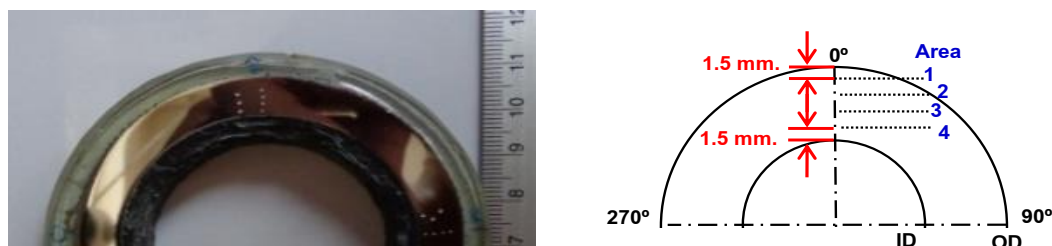


Figure 2. The location on the cross section of tube specimen for micro-hardness testing.

All specimens were cut into smaller pieces and then mounted into Bakelite cylinders. Thereafter, the specimen's surfaces were polished by using abrasive SiC paper (No. 120, 240, 400, 600, 800 and 1000). After every step of polishing, the surfaces were etched in mixed solutions (40 mL glycerol, 20 mL HCl and 20% HNO₃). Additionally, the specimens were cleaned in an ultrasonic bath. Lastly, the SEM-BSE combined with EDS mapping were used to analyze the microstructure and elemental composition.

3. Results and Discussion

3.1. Material Verification

A visual inspection of Specimen No. 1 found that it had no significant internal or external damage. It showed a good quality of structures with no visible pits, no deposit and no signs of carburization. On the other hand, carburization reactions and coke deposits were observed at different configurations in the three height positions studied. Specimen No. 2 had the most coke deposits and signs of carburization, but also a roundness and shape that was significantly more deformed than Specimens No. 3 and No. 4, respectively. However, no cracking in Specimens No. 2, No. 3 or No. 4 were observed (Table 2).

Figure 3 shows the XRD patterns of the Cr-Ni-Nb alloy before and after use in the pyrolysis furnace. Specimen No. 1 exhibited both diffraction peaks corresponding to the γ' austenitic (FCC) phase and the γ'' (BCT) phase of Cr-Ni-Nb alloy and Ni₃Nb, respectively, as shown in Figure 3a. In the case of Specimen No. 2, the XRD pattern (Figure 3b) displayed the same major peaks of FCC and BCT phases as the new tube. Moreover, Specimen No. 2 exhibited the additional peaks which correspond to the carbide structures of NbC (JCPDS No. 00-038-1364), SiC (JCPDS No. 000-029-1129) and Cr₂₃C₆ (JCPDS No. 00-035-0783). This result clearly indicated that the precipitated carbide of the tube furnace was produced in the process of ethane pyrolysis.

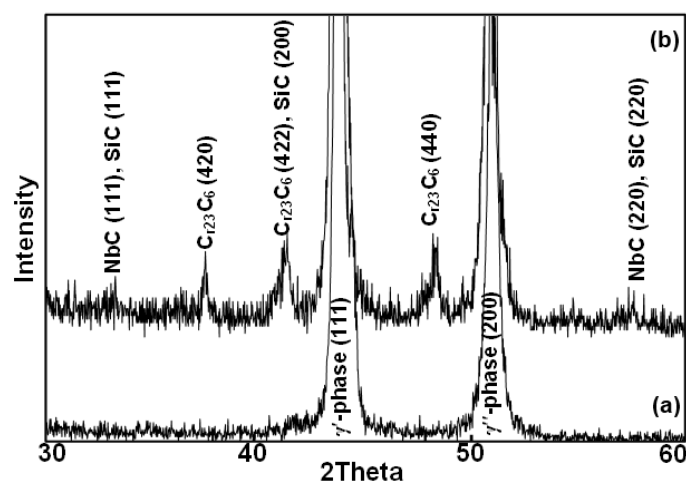


Figure 3. XRD patterns of (a) the new tube and (b) the used tube.

The microstructure of the Cr-Ni-Nb alloy and its carbide was observed by SEM-BSE and EDS mapping, as shown in Figure 4. BSE is the electron signal from elastic scattering interaction between electron beam and atomic specimen. This interaction depends on the atomic weight of the atom. The more heavy an atom is, the more a BSE signal can be generated, giving results in a brighter contrast. Therefore, the BSE is used to detect contrasts between areas with different elemental compositions [19,20]. Figure 4a,b shows the backscattered electrons images (BEI) of Specimen No. 1 (the new tube), in which three different phases (bright, gray and dark) are found. The Nb, a heavy element (high atomic number), exhibited more BSE than those of the lighter elements (low atomic number), and thus appeared brighter in BEI. The gray area was identified as the major part of the matrix alloy, while the dark area in BEI might be the precipitated carbide.

By elemental analysis, the EDS mapping (Figure 4c–h) of Specimen No. 1 confirmed a good dispersion of elementals in the alloy. The EDS revealed that the results agreed to XRD, and that the matrix (Ni-Cr-Fe solid solution) was observed as γ austenitic (FCC), with a variety of secondary phases of γ'' -Ni₃Nb (BCT), a strengthener phase comprised of an austenite matrix. The small numbers of coarse chromium carbide precipitates were observed within the matrix and at grain boundaries. Moreover, the mapping of Cr (Figure 4f) was found to be similar to the dark area in BEI (Figure 4b), which indicated that the chromium and carbon appeared as a small chromium carbide precipitation. However, this carbide phase cannot be observed in XRD because of the detection limit of the XRD technique.

In the case of one of the used tubes (Specimen No. 2), the BEI and EDS (Figure 4i–p) showed the microstructure of the austenite matrix and more Cr-rich carbides (Figure 4n). Moreover, a phase separation of mixed NbC and SiC was found, shown in Figure 4l,p. The obtained results of XRD and SEM-BSE with EDS confirmed that the pyrolysis caused the carbide precipitation in the microstructure of the Cr-Ni-Nb alloy. The carbide precipitate decreased the tensile strength, creep resistance and corrosion resistance, and increased the brittle fracture property, the hardness, and the ductility of the material [21].

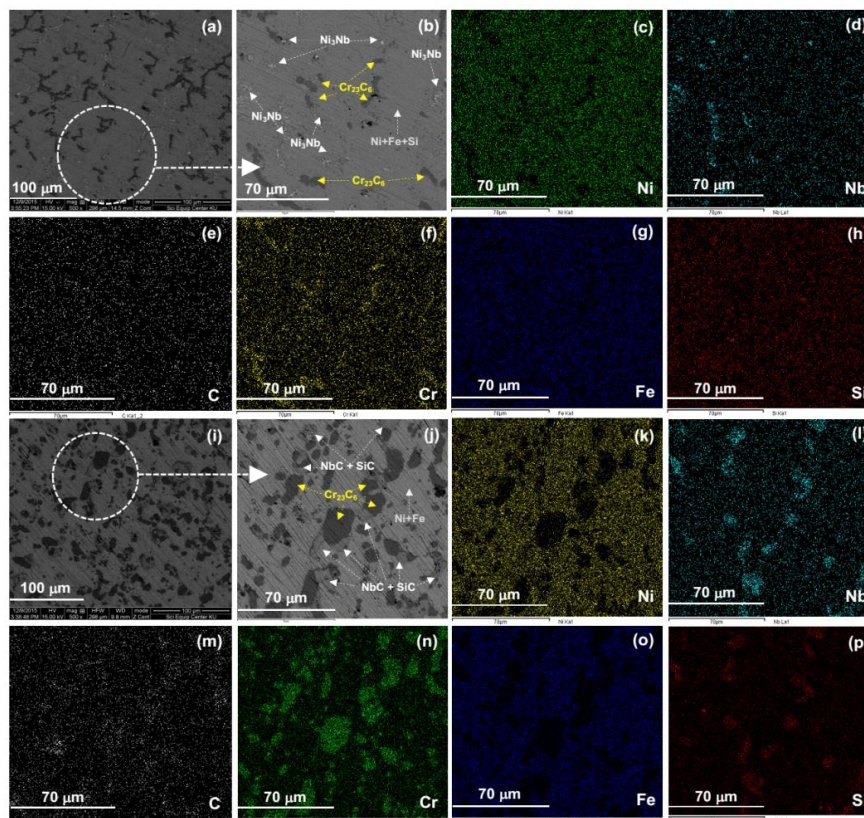


Figure 4. BEI and EDS mapping of (a–h) Specimen No. 1 (new); and (i–p) Specimen No. 2 (used).

3.2. Heat Treatment, Hardness and Microstructure

The hardness of specimens before (No. 1) and after heat treatment (No. 2–4) in four areas were tested and compared, as shown in Figure 5.

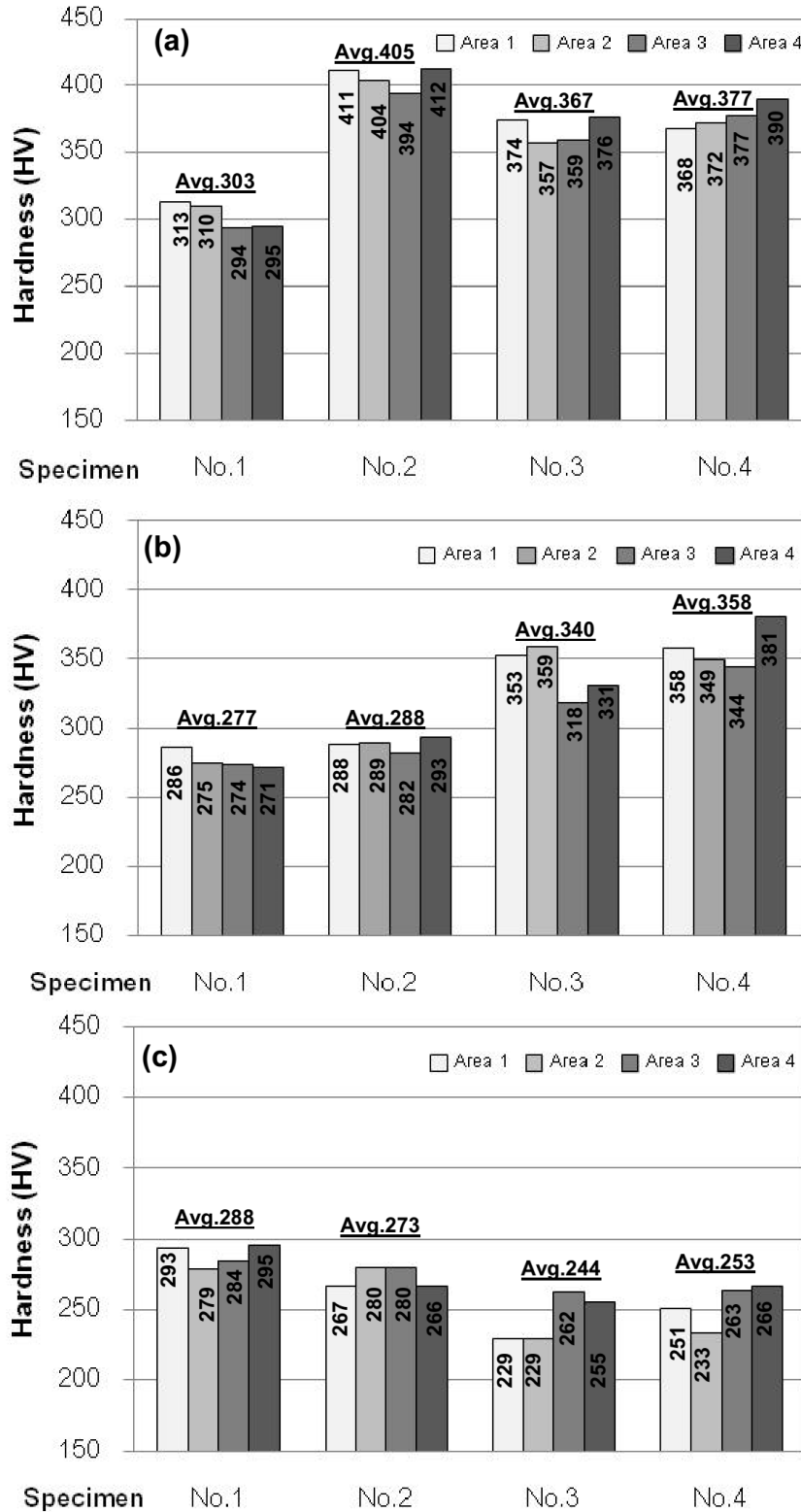


Figure 5. The hardness value of four areas in each specimen with different heat treatments: (a) without heat treatment; (b) 600 °C/1 h; and (c) 900 °C/1 h.

Figure 5 presents the hardness of each specimen with various heat treatment conditions. Each bar shows the hardness value averaged from two readings at four different positions on a cross section of specimens. In condition C1 (without heat treatment), the lowest hardness value was observed in Specimen No. 1 with an average value of 303 HV, as shown in Figure 5a. On the other hand, Specimen No. 2 with thick coke deposit inside the wall of a higher position of the pyrolysis furnace had the highest hardness value, average as 405 HV. However, the average hardness was reduced to 377 HV and 367 HV for Specimen No. 4 and No. 3, respectively.

In Figure 5b, the effect of the heat treatment process showed a considerable decrease in the hardness value of all specimens. In the case of condition C2 (annealing 600 °C, 1 h/air cooled), the average hardness values decreased to 288, 340 and 358 HV for Specimens No. 2–4, respectively. However, the annealing temperature of condition C2 was within the range of sensitization, so chromium carbide could be precipitated at grain boundary. Therefore, the hardness values of used tube specimens were still greater and higher than that of Specimen No. 1 (average of 277 HV). In addition, Specimen No. 2 was acquired from the top part of the furnace tube, where the high carbon content was accumulated as coke and tended to form a large amount of carbide phase. Therefore, the significant decrease of hardness in sample 2 after heat treatment at 600 °C might be due to the superior loss of these carbide grains when compared to those of Specimens No. 3–4.

Relating to condition C3 (annealing 900 °C, 1 h/air cooled), as shown in Figure 5c, the lowest hardness values were determined to be 273, 244 and 253 HV for Specimens 2–4, respectively, when compared to the heat treatment condition of C1 and C3. The hardness measurement indicated that condition C3 was a suitable condition because it could change the hardness values of the used tubes close to the new tube for avoiding cracking damage during the weld repair and can be used to improve the weldability of 35Cr-45Ni-Nb alloy.

Furthermore, SEM/EDS analysis could confirm a significant reason for a using thermal heat treatment to a 35Cr-45Ni-Nb used tube for welding repair. The microstructures of each specimen at heat treatment conditions of C2 and C3 by using SEM/EDS mapping are shown in Figures 6 and 7 respectively.

In Figure 6a, after heat treatment, Specimen No. 1 showed that the white precipitate adjacent to the grain boundaries was Nb-rich in the metastable γ'' -Ni₃Nb phase as shown by EDS mapping. Whereas, a small number of chromium carbide precipitates were observed within the matrix and at the grain boundaries. Thus, it could be suggested that the good mechanical properties were exhibited because the phase transformation could not be observed in the microstructure of Specimen No. 1.

Figure 6b–d shows the microstructures in the used tube specimen. Specimens No. 2 and No. 3 also revealed coarse chromium carbide precipitation and a continuous carbide lattice at austenite grain boundaries, while the metastable γ'' -Ni₃Nb phase could not be observed in the matrix austenite. Additionally, the SiC and NbC were separated from the matrix austenite, which corresponded to the degree of hardness values. The microstructure of Specimen No. 4 showed small amounts of SiC and NbC within the area of chromium carbide precipitation at grain boundaries. This could be explained by the laws of thermodynamic and the Gibbs free energy such that the significant alloying elements (such as Nb and Si) were quickly activated with carbon atoms and reduced the degree of sensitization [15,21–23]. Therefore, it could be recommended that condition C2 (annealing 1 h (600 °C)/air cooled) could not give a beneficial effect to ensure that the precipitation of Cr₂₃C₆ was dissolved properly in the used tube for repair welding procedure.

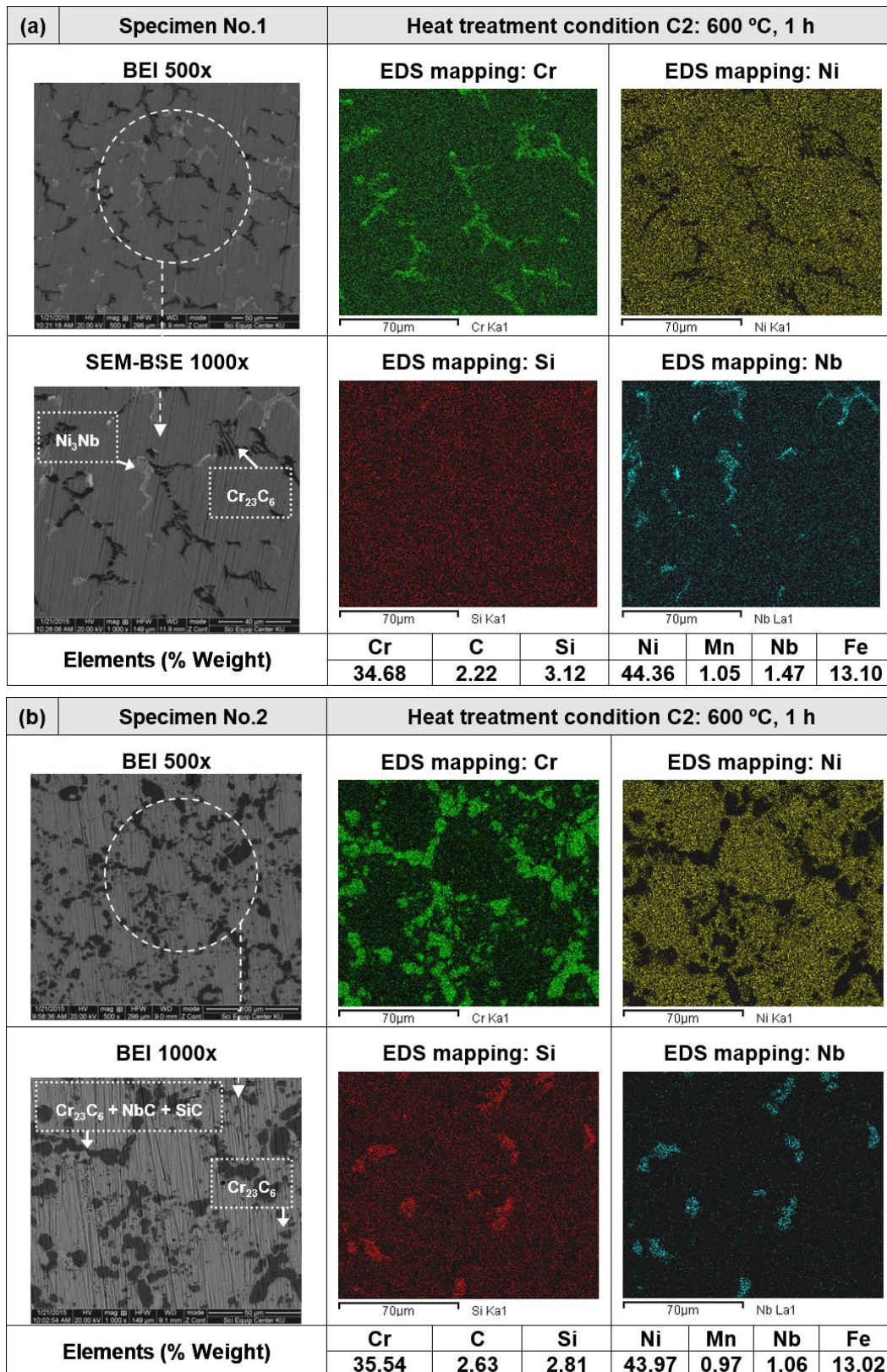


Figure 6. Cont.

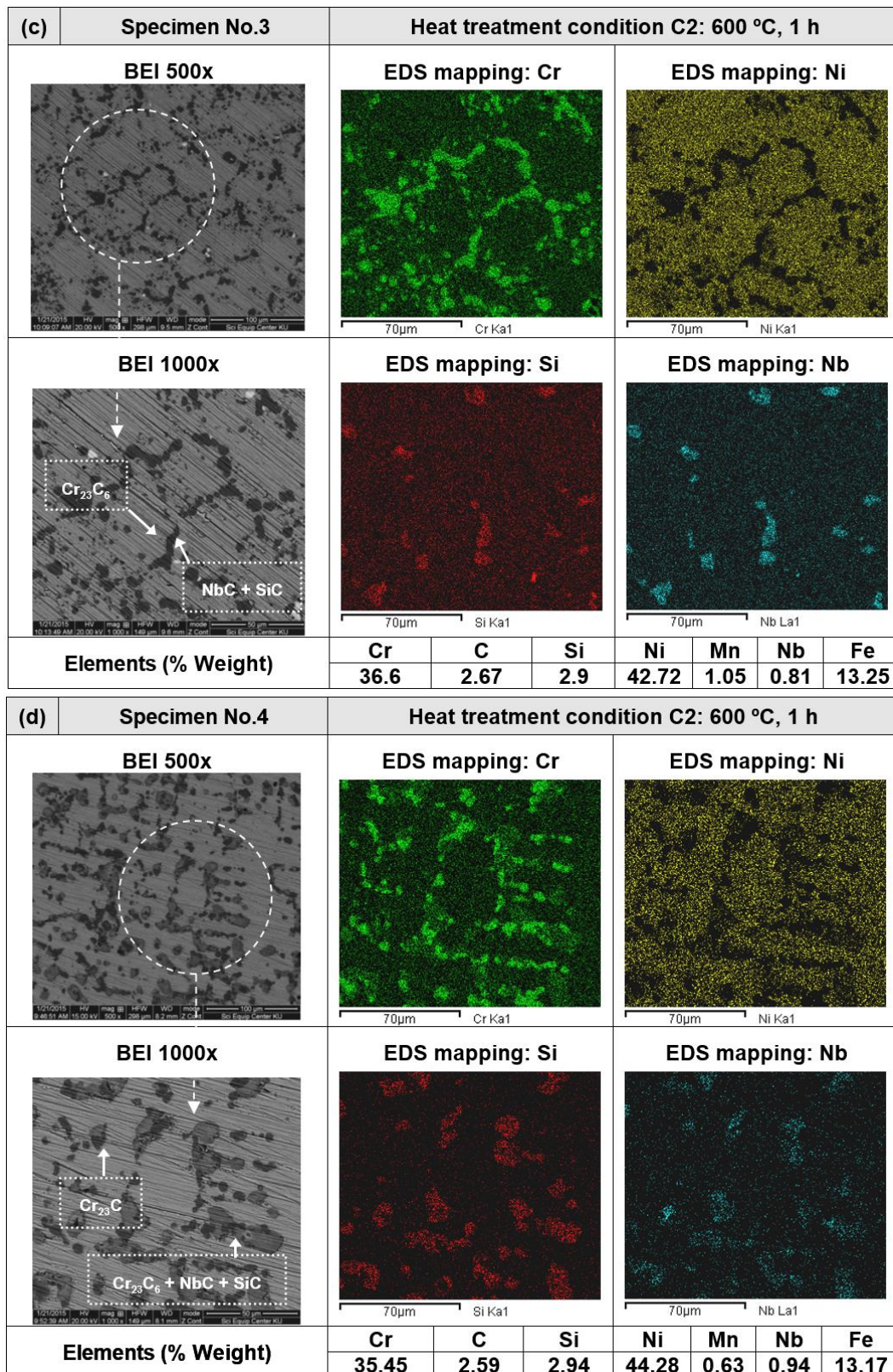


Figure 6. BEI and EDS mapping of the 35Cr-45Ni-Nb specimens after 1 h of thermal heat treatment at 600 °C: (a) Specimen No. 1; (b) Specimen No. 2; (c) Specimen No. 3; (d) Specimen No. 4.

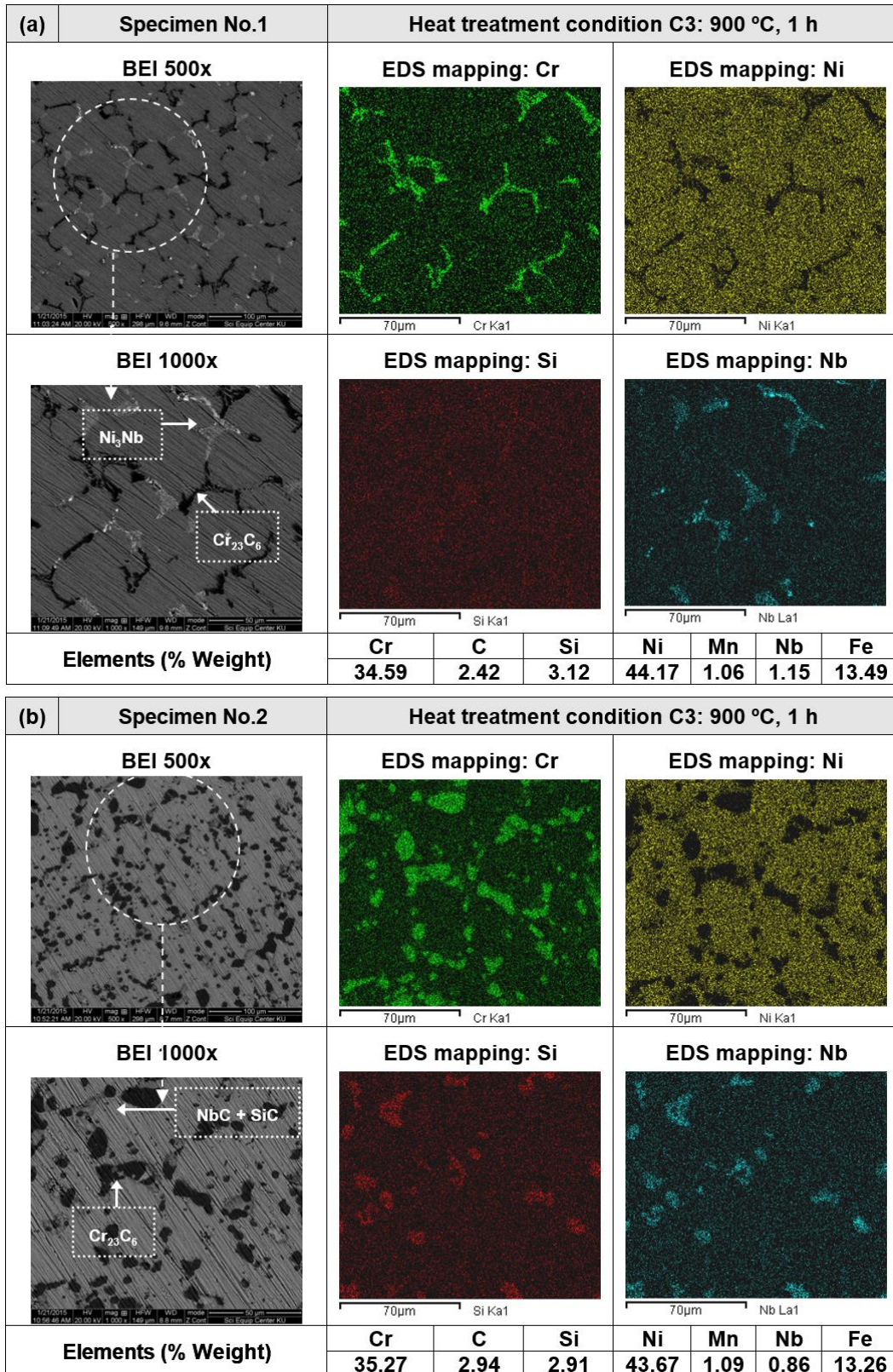


Figure 7. Cont.

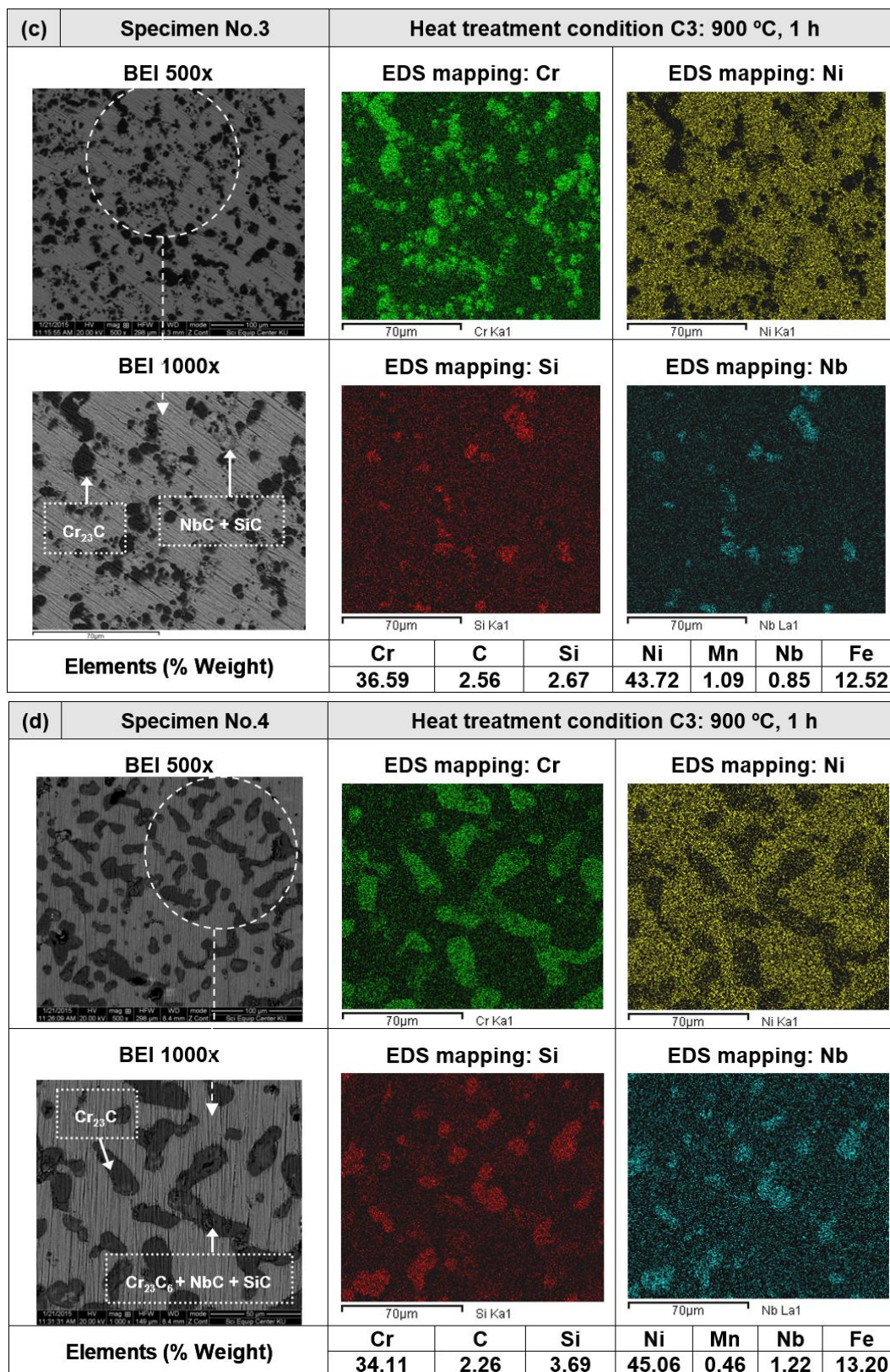


Figure 7. BEI and EDS mapping of the 35Cr-45Ni-Nb specimens after 1 h of thermal heat treatment at 900 °C: (a) Specimen No. 1; (b) Specimen No. 2; (c) Specimen No. 3; (d) Specimen No. 4.

In condition C3, the formation of the metastable γ'' -Ni₃Nb phase occurred in the austenite matrix, as shown in Figure 7a. However, the degree of sensitization at grain boundaries was enlarged when compared to Specimen No. 1 in the condition C2. This was due to the fact that, after annealing at high temperature of 900 °C, the higher cooling rate could increase the reverse transformation of carbide particles [24].

Figure 7b–d shows the microstructure of carbide precipitates. It was found that the particles of chromium carbide were dispersed and discontinued in the matrix austenite, and the small particles of SiC and NbC occurred in the area of chromium carbides precipitation. In addition, there might be other factors affecting the hardness, such as the redistribution of the phase component in the alloy, particularly Ni, Si and Nb phases. Therefore, the mechanical properties and weldability of used tube specimens were enhanced.

As a result, it is suggested that condition C3 (annealing 900 °C 1 h/air cooled) was a suitable method for chromium carbides dissolution which help decreased the hardness values of the used tubes and might improved the weldability of furnace tube repair.

4. Conclusions

The aim of this work was to find an suitable heat treatment process to decrease the hardness value and/or reduce the chromium carbide precipitation at grain boundary of material due to the major problem in welding repair of ethylene pyrolysis tubes, a dissimilar material between used tubes and new tubes. This experiment confirmed the carburization in the 35Cr-45Ni-Nb alloy tube after long-term service at high temperature in an ethylene pyrolysis furnace. The carbide precipitation at grain boundary of the austenite matrix was found to increase the hardness values of the specimen. However, after thermal heat treatment (annealing 900 °C 1 h/air cooled), a decrease in the carbide precipitate in the austenite matrix and in the hardness value of each specimen was observed when compared to those before heat treatment. The temperature range and cooling rate were important influences for the dissolution of carbides and reverse transformation. Furthermore, the next study will investigate parameters which are significant for the successful joints of furnace tube repair, such as wire electrode, welding process and post-weld heat treatment in the welding procedures.

Acknowledgments: This research was funded by King Mongkut's University of Technology North Bangkok (Contract No. KMUTNB-GEN-57-55). The authors are very grateful to IRPC Public Company Limited for supporting information and materials that used in this experiment. Additionally, thanks to Chockchai Singhatham, in support of sample preparation for hardness testing.

Author Contributions: N. Srisuwan performed reseach and wrote the article. K. Eidhed and N. Kreatsereekul helped in the experimental part. T. Yingsamphancharoen and A. Kaewvilai assisted in the material characterization, data analysis and revised manuscript.

Conflicts of Interest: The authors declare no conflict of interest.

References

1. Ul-Hamid, A.; Tawancy, H.M.; Al-Jaroudi, S.S.; Mohammed, A.I.; Abbas, N.M. Carburisation of Fe-Ni-Cr alloys at High Temperatures. *Mater. Sci. Pol.* **2006**, *24*, 219–331.
2. Grabke, H.J. Carburization, Carbide Formation, Metal Dusting, Coking. *J. Mater. Technol.* **2002**, *36*, 297–305.
3. Babakr, A.; Habiby, F. Lengthening, Cracking and Weld ability Problems of Fe-Ni-Cr Alloy Tube. *J. Miner. Mater. Charact. Eng.* **2009**, *8*, 133–148.
4. Verdier, G.; Carpentier, F. Consider New Materials for Ethylene Furnace Applications. *Hydrocarb. Process.* **2011**, *90*, 61–62.
5. Raghavan, V. Cr-Fe-Ni (Chromium-Iron-Nickel), Section II: Phase Diagram Evaluations. *J. Phase Equilib. Diffus.* **2009**, *30*, 94–95. [[CrossRef](#)]
6. Davis, J.R. *ASTM Specially Handbook: Heat-Resistant Materials*; ASM International: Novelty, OH, USA, 1997; p. 224.

7. Yang, Z.G.; Paxton, D.M.; Weil, K.S.; Stevenson, J.W.; Singh, P. *Materials Properties Database for Selection of High-Temperature Alloys and Concepts of Alloy Design for SOFC Applications*; Pacific Northwest National Laboratory: Richland, WA, USA, 2002.
8. Shatynski, S.R. The Thermochemistry of Transition Metal Carbides. *Oxid. Met.* **1979**, *13*, 105–118. [[CrossRef](#)]
9. Rashid, M.W.A.; Gakim, M.; Rosli, Z.M.; Azam, M.A. Formation of Cr₂₃C₆ during the Sensitization of AISI 304 Stainless Steel and its Effect to Pitting Corrosion. *Int. J. Electrochem. Sci.* **2012**, *7*, 9465–9477.
10. Durand-Charre, M. *Microstructure of Steels and Cast Irons*; E-Book: New York, NY, USA, 2004.
11. Avery, R.E.; Tuthill, A.H. *Guidelines for the Welded Fabrication of Nickel Alloys for Corrosion-Resistance Service*; The Nickel Development Institute: Toronto, ON, Canada, 1994; p. 22.
12. Punburi, P.; Tareelap, N. Post Weld Heat Treatment to Reduce Intergranular Corrosion Susceptibility of Dissimilar Welds Between Austenitic 304 and Ferritic 430 Stainless Steels. In Proceedings of the 1st Mae Fah Luang University International Conference, Bangkok, Thailand, 29 November–1 December 2012; pp. 1–9.
13. Singhatham, C.; Srisuwan, N.; Intho, R.; Theerawatanchai, N.; Pitiariyanan, K.; Eidhed, K. Root Cause Analysis of the Carburized 35Cr-45Ni-Nb Tube in the Ethylene Furnace. *J. Appl. Sci. Res.* **2003**, *9*, 5999–6009.
14. Chasselin, H. Carburization in Ethylene Radiant Coils. AIChE Paper No. 295746. In Proceedings of the 2013 Spring National Meeting, San Antonio, TX, USA, 28 April–2 May 2013.
15. Loto, C.A. Microstructural Analysis of Ethylene Furnace Steel Alloy Tubes. *Mater. Perform. NACE Int.* **2011**, *50*, 2–8.
16. Takcuchi, Y.; Kato, Y.; Yokota, N.; Tsuchiya, M.; Shimizu, T.; Tanaka, I. Multi-Layered Anti-Coking Heat Resistant Metal Tube and Method for Manufacture Thereof. U.S. Patent 6,337,459 B1, 8 January 2002.
17. Kennedy, R. Life Improvement of Alloys in Heat Treatment Furnaces and Fixtures. In *Degree of Bachelor of Science in Mechanical Engineering*; Worcester Polytechnic Institute: Worcester, MA, USA, 2013.
18. Dossett, J.L.; Boyer, H.E. *Practical Heat Treating*, 2nd ed.; ASM International: Novelt, OH, USA, 2006.
19. Wells, O.C.; Gordon, M.S.; Gignac, L.M. Past, Present, and Future of Backscatter Electron (BSE) Imaging. *Proc. SPIE* **2012**. [[CrossRef](#)]
20. Santos, M.; Guedes, M.; Baptista, R.; Infante, V.; Cláudio, R.A. Effect of severe operation conditions on the degradation state of radiant coils in pyrolysis furnaces. *Eng. Fail. Anal.* **2015**, *56*, 194–203. [[CrossRef](#)]
21. Shao, G. Thermodynamic Modeling of the Cr-Nb-Si System. *J. Intermet.* **2005**, *13*, 69–78. [[CrossRef](#)]
22. Serna, A.; Rapp, R.A. Carburization of Austenitic and Ferritic Alloys in Hydrocarbon Environments at High Temperature. *J. Rev. Metal. Madrid* **2003**, *39*, 162–166. [[CrossRef](#)]
23. Marinkovic, B.A.; Avillez, R.R.; Barros, S.K.; Assunção, F.C.R. Thermodynamic Evaluation of Carbide Precipitates in 2.25Cr-1.0Mo Steel for Determination of Service Degradation. *J. Mater. Res.* **2002**, *5*, 491–495. [[CrossRef](#)]
24. Xu, M.L. Secondary carbide dissolution and coarsening in 13% Cr martensitic stainless steel during austenitizing. In *Mechanical Engineering Dissertations*; Northeastern University: Boston, MA, USA, 2012.

